



Inhibition of Ammonia Monooxygenase from Ammonia-Oxidizing Archaea by Linear and Aromatic Alkynes

Chloë L. Wright,^a Arne Schatteman,^a Andrew T. Crombie,^a J. Colin Murrell,^b Laura E. Lehtovirta-Morley^a

^aSchool of Biological Sciences, University of East Anglia, Norwich, United Kingdom

^bSchool of Environmental Sciences, University of East Anglia, Norwich, United Kingdom

ABSTRACT Ammonia monooxygenase (AMO) is a key nitrogen-transforming enzyme belonging to the same copper-dependent membrane monooxygenase family (CuMMO) as the particulate methane monooxygenase (pMMO). The AMO from ammonia-oxidizing archaea (AOA) is very divergent from both the AMO of ammonia-oxidizing bacteria (AOB) and the pMMO from methanotrophs, and little is known about the structure or substrate range of the archaeal AMO. This study compares inhibition by C₂ to C₈ linear 1-alkynes of AMO from two phylogenetically distinct strains of AOA, “*Candidatus Nitrosocosmicus franklandus*” C13 and “*Candidatus Nitrosotalea sinensis*” Nd2, with AMO from *Nitrosomonas europaea* and pMMO from *Methylococcus capsulatus* (Bath). An increased sensitivity of the archaeal AMO to short-chain-length alkynes (\leq C₅) appeared to be conserved across AOA lineages. Similarities in C₂ to C₈ alkyne inhibition profiles between AMO from AOA and pMMO from *M. capsulatus* suggested that the archaeal AMO has a narrower substrate range than *N. europaea* AMO. Inhibition of AMO from “*Ca. Nitrosocosmicus franklandus*” and *N. europaea* by the aromatic alkyne phenylacetylene was also investigated. Kinetic data revealed that the mechanisms by which phenylacetylene inhibits “*Ca. Nitrosocosmicus franklandus*” and *N. europaea* are different, indicating differences in the AMO active site between AOA and AOB. Phenylacetylene was found to be a specific and irreversible inhibitor of AMO from “*Ca. Nitrosocosmicus franklandus*,” and it does not compete with NH₃ for binding at the active site.

IMPORTANCE Archaeal and bacterial ammonia oxidizers (AOA and AOB, respectively) initiate nitrification by oxidizing ammonia to hydroxylamine, a reaction catalyzed by ammonia monooxygenase (AMO). AMO enzyme is difficult to purify in its active form, and its structure and biochemistry remain largely unexplored. The bacterial AMO and the closely related particulate methane monooxygenase (pMMO) have a broad range of hydrocarbon cooxidation substrates. This study provides insights into the AMO of previously unstudied archaeal genera, by comparing the response of the archaeal AMO, a bacterial AMO, and pMMO to inhibition by linear 1-alkynes and the aromatic alkyne, phenylacetylene. Reduced sensitivity to inhibition by larger alkynes suggests that the archaeal AMO has a narrower hydrocarbon substrate range than the bacterial AMO, as previously reported for other genera of AOA. Phenylacetylene inhibited the archaeal and bacterial AMOs at different thresholds and by different mechanisms of inhibition, highlighting structural differences between the two forms of monooxygenase.

KEYWORDS ammonia monooxygenase, ammonia oxidizers, inhibition, linear 1-alkynes, methanotrophs, phenylacetylene

Nitrification is a key microbial process in the global nitrogen cycle. Autotrophic archaeal and bacterial ammonia oxidizers (AOA and AOB, respectively) and commammox bacteria, which carry out the complete oxidation of ammonia to nitrate (1, 2),

Citation Wright CL, Schatteman A, Crombie AT, Murrell JC, Lehtovirta-Morley LE. 2020. Inhibition of ammonia monooxygenase from ammonia-oxidizing archaea by linear and aromatic alkynes. *Appl Environ Microbiol* 86:e02388-19. <https://doi.org/10.1128/AEM.02388-19>.

Editor Alfons J. M. Stams, Wageningen University

Copyright © 2020 Wright et al. This is an open-access article distributed under the terms of the [Creative Commons Attribution 4.0 International license](https://creativecommons.org/licenses/by/4.0/).

Address correspondence to Laura E. Lehtovirta-Morley, l.lehtovirta-morley@uea.ac.uk.

Received 18 October 2019

Accepted 15 February 2020

Accepted manuscript posted online 21 February 2020

Published 17 April 2020

initiate nitrification through the oxidation of ammonia (NH_3) to hydroxylamine (NH_2OH), a reaction catalyzed by ammonia monooxygenase (AMO). AMO is the only enzyme of the ammonia oxidation pathway which is shared by all three major groups of ammonia oxidizers (3). Quantitative assessments based on the *amoA* gene, which encodes the AmoA subunit of AMO, have revealed that AOA are ubiquitous in the environment and are among the most numerous living organisms on Earth, often outnumbering AOB in many environments where nitrification occurs (4–7). Environmental surveys using *amoA* as a marker gene have been crucial for our understanding of the distribution and diversity of AOA; however, little is known about the structure or biochemistry of the archaeal AMO and how this differs from that of AOB.

AMO is a copper-dependent multimeric transmembrane enzyme belonging to the copper-dependent membrane monooxygenase (CuMMO) superfamily, which comprises ammonia, methane, and alkane monooxygenases (7–9). Members of the CuMMO family have a broad substrate range, and it has been suggested that subsequent metabolic steps define the functional role of microbes containing CuMMO (10, 11). For example, the AOB *Nitrosomonas europaea* and *Nitrosococcus oceani* can oxidize methane but lack necessary downstream enzymes to gain reducing power from methane oxidation (12, 13). Likewise, the particulate methane monooxygenase (pMMO) of methanotrophs can cooxidize NH_3 (14–16) as well as various hydrocarbons, for instance, linear 1-alkanes (C_2 to C_5) and alkenes (C_2 to C_4) (17–19), and halogenated hydrocarbons (20), but none of these oxidation substrates can support growth. The bacterial AMO has a broader substrate range than the pMMO and is capable of cooxidizing 1-alkanes (C_2 to C_8) and alkenes (C_2 to C_5) (21), halogenated hydrocarbons (22, 23), aromatic compounds (24), and sulfides (25, 26) to yield oxidized products. Difficulties in purifying active AMO limit the amount of structural data available, and many predictions about the structure of AMO are based on homology to the pMMO (8, 10, 27, 28). However, the pMMO itself has proven challenging to fully characterize, and the nature and location of the sites of O_2 activation and methane oxidation remain uncertain. To date, a diiron site located on the PmoC subunit (29), and multiple copper sites of different nuclearities located on separate subunits (PmoA, PmoB, and PmoC) have all been suggested as potential active sites (27, 30–34).

Insights regarding the structure and function of AMO have largely come from whole-cell studies investigating its interaction with both reversible and irreversible inhibitors. For example, the bacterial AMO is inhibited by the copper chelator allylthiourea (ATU), which strongly indicates that it is a copper-dependent enzyme (18, 35–38). Acetylene is a well-characterized inhibitor of both AMO and pMMO (39–41). With *N. europaea*, acetylene acts as a suicide substrate, and cells require *de novo* protein synthesis of new AMO to reestablish NH_3 -oxidizing activity (42). Incubations with [^{14}C]acetylene resulted in the covalent radiolabeling of *N. europaea* AMO, enabling identification of the genes coding for AMO (41, 43). A subsequent study found that the ketene product of acetylene activation bound covalently to a histidine residue (H191) in the AmoA subunit of *N. europaea*, a residue thought to be in the proximity of the AMO active site (44). While acetylene is also an irreversible inhibitor of the archaeal AMO, the AMOs from archaea lack the histidine residue responsible for binding in *N. europaea*, suggesting that the product of acetylene oxidation must bind at a different position on the enzyme. AMO from *N. europaea* is also irreversibly inhibited by other terminal and subterminal alkynes, including C_3 to C_{10} 1-alkynes (21), 3-hexyne (45) and 1,7-octadiyne (46). Interestingly, in *N. europaea*, the degree of inhibition by 1-alkynes, as a function of chain length, inversely mirrors the activity with the corresponding 1-alkanes (21).

Virtually nothing is known about the substrate range of the archaeal AMO. Previously, Taylor et al. (47, 48) showed that in whole-cell studies, aliphatic *n*-alkynes (C_2 to C_9) differentially inhibited bacterial and archaeal AMOs, with AOA being less sensitive to $\geq\text{C}_5$ 1-alkynes. Inhibition of AMO by 1-octyne (C_8) has since been used in environmental and mesocosm studies to discriminate between the contributions of AOA and AOB to soil nitrification (49–52). A field study by Im et al. (53) showed that the

abundance of archaeal *amoA* genes decreased when the soil was treated with the aromatic alkyne phenylacetylene, although the effects of phenylacetylene on pure cultures of AOA were not investigated. Phenylacetylene was shown to be a strong inhibitor of the AMO from *N. europaea* (41), with complete inhibition at $<1 \mu\text{M}$ (54), and the AMO from *N. europaea* is capable of oxidizing aromatic compounds, including the alkane analogue of phenylacetylene, ethylbenzene (24, 55). Interestingly, the oxidation of aromatic hydrocarbons has not been observed for the pMMO (17, 21, 40, 56).

The initial aim of this study was to undertake a comprehensive assessment of the inhibition of archaeal AMO activity by C_2 to C_8 linear 1-alkynes using two terrestrial AOA strains from distinct thaumarchaeal lineages, "*Candidatus Nitrosocosmicus franklandus*" C13 and "*Candidatus Nitrosotalea sinensis*" Nd2. 1-Alkyne inhibition profiles of *N. europaea* AMO and the pMMO from *Methylococcus capsulatus* (Bath) were also investigated for comparison. For consistency and to provide a direct comparison with AMO, the inhibition of NH_3 -oxidizing activity by the pMMO from *M. capsulatus* (Bath) was investigated. NH_3 is a cometabolic substrate of the pMMO from *M. capsulatus* (Bath) and is oxidized to hydroxylamine, which is further oxidized to produce NO_2^- (14, 57).

Next, phenylacetylene inhibition profiles of NH_3 oxidation by "*Ca. Nitrosocosmicus franklandus*" and *N. europaea* cells were compared. The kinetic mechanism of inhibition of intact cells of "*Ca. Nitrosocosmicus franklandus*" and *N. europaea* by phenylacetylene was investigated to explore differences in the biochemistry of the archaeal and bacterial AMOs. Evidence from previous studies suggests that NH_3 , rather than ammonium (NH_4^+), is the growth substrate oxidized by the bacterial AMO (58), but the preferred substrate ($\text{NH}_3/\text{NH}_4^+$) oxidized by the archaeal AMO has not been determined. However, it is highly likely to also be NH_3 based on archaeal and bacterial AMO sequence comparisons (59). At the pH of the systems used here, the majority of the NH_3 (pK_a of 9.25) would be protonated. Therefore, calculations of kinetic parameters presented in this study are based on total reduced inorganic nitrogen (NH_3 plus NH_4^+) as the substrate.

RESULTS

Sensitivity of "*Ca. Nitrosocosmicus franklandus*," "*Ca. Nitrosotalea sinensis*," *N. europaea*, and pMMO-expressing *M. capsulatus* (Bath) to C_2 to C_8 1-alkynes. The sensitivity of intact "*Ca. Nitrosocosmicus franklandus*" and "*Ca. Nitrosotalea sinensis*" cells to $10 \mu\text{M}$ aqueous concentrations (C_{aq}) of C_2 to C_8 1-alkynes was compared to those of *N. europaea* and the pMMO-expressing methanotroph, *M. capsulatus* (Fig. 1). NH_3 -dependent NO_2^- production by both "*Ca. Nitrosocosmicus franklandus*" and "*Ca. Nitrosotalea sinensis*" was inhibited by C_2 to C_5 1-alkynes ($P < 0.001$) but not by C_7 and C_8 (Fig. 1A and B). "*Ca. Nitrosotalea sinensis*" was strongly inhibited by C_4 and C_5 alkynes (degrees of inhibition, $54\% \pm 5\%$ and $70\% \pm 1\%$, respectively, compared with that of controls); however, these alkynes effected only partial inhibition of NH_3 oxidation by "*Ca. Nitrosocosmicus franklandus*" ($24\% \pm 2\%$ and $14\% \pm 1\%$, respectively), indicating differences in the alkyne sensitivities of different AOA strains. Additionally, 1-hexyne had a significant inhibitory effect on "*Ca. Nitrosotalea sinensis*" ($P = 0.004$) but not on "*Ca. Nitrosocosmicus franklandus*" ($P = 0.47$). NO_2^- production by *N. europaea* was strongly inhibited by all 1-alkynes tested (C_2 to C_8). 1-Pentyne resulted in $98\% \pm 1\%$ inhibition, and AMO activity was completely inhibited by C_6 to C_8 1-alkynes (Fig. 1C). In the presence of C_3 and C_4 1-alkynes, inhibition decreased to $78\% \pm 1\%$ and $54\% \pm 1\%$, respectively. pMMO-expressing *M. capsulatus* cells oxidized NH_4^+ to NO_2^- , and NO_2^- production was significantly inhibited by C_2 to C_7 1-alkynes ($P \leq 0.001$), but C_6 and C_7 1-alkynes resulted in only approximately 10% inhibition compared with that of the control (Fig. 1D). NO_2^- production from NH_3 by the pMMO from *M. capsulatus* is shown in Fig. S1 in the supplemental material. The rate of NO_2^- production decreased after 1 h of incubation, likely due to the toxic buildup of NO_2^- and hydroxylamine in the culture.

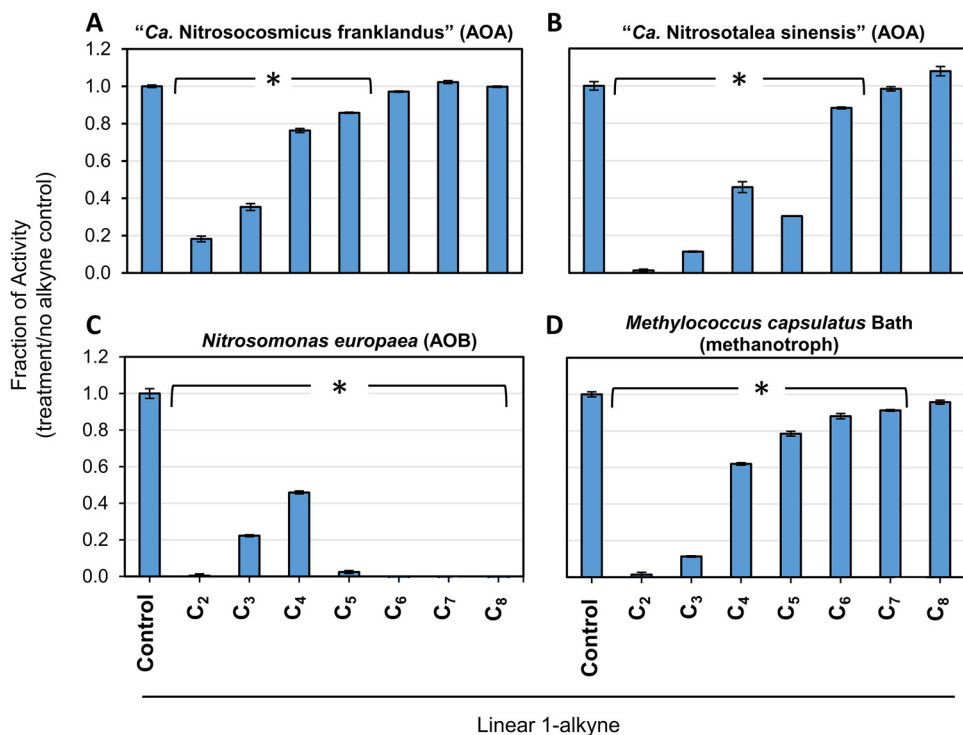


FIG 1 Inhibition of NO₂⁻ production by “*Ca. Nitrosocosmicus franklandus*” (A), “*Ca. Nitrosotalea sinensis*” (B), *N. europaea* (C), and *M. capsulatus* (Bath) (D) in response to 10 μM (C_{aq}) C₂ to C₈ 1-alkynes. *N. europaea*, “*Ca. Nitrosocosmicus franklandus*,” and “*Ca. Nitrosotalea sinensis*” were incubated with 1 mM NH₄⁺ and *M. capsulatus* (Bath) with 20 mM NH₄⁺. Error bars represent standard errors (SEs) of the means (n = 3). *, 1-alkyne treatments that significantly inhibited NO₂⁻ production relative to the control treatment (P < 0.01).

Notably, “*Ca. Nitrosotalea sinensis*,” *N. europaea*, and *M. capsulatus* (Bath) were very sensitive to 10 μM acetylene (C₂), with NO₂⁻ production inhibited by >95%; however, “*Ca. Nitrosocosmicus franklandus*” appeared less sensitive to acetylene (degree of inhibition, 82% ± 3%).

Inhibition of NO₂⁻ production by “*Ca. Nitrosocosmicus franklandus*” and *N. europaea* in response to phenylacetylene. Given the contrasting responses of ammonia-oxidizing archaea and bacteria to linear alkynes, AMO activity in the presence of the aromatic alkyne phenylacetylene was examined in “*Ca. Nitrosocosmicus franklandus*” and *N. europaea* cells (Fig. 2). After 1 h of incubation, the rate of NH₃-dependent

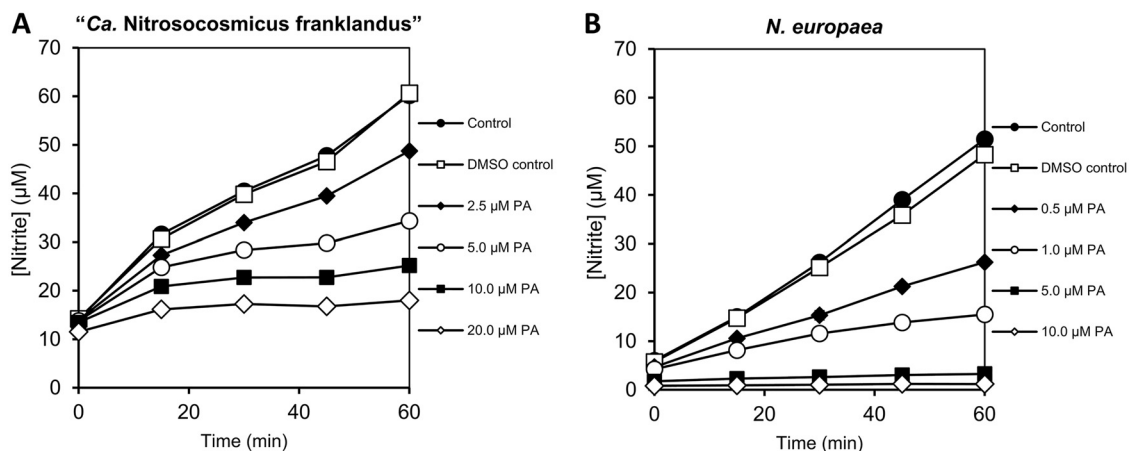


FIG 2 NO₂⁻ production by “*Ca. Nitrosocosmicus franklandus*” (A) and *N. europaea* (B) in response to different concentrations of phenylacetylene (PA) dissolved in DMSO. Error bars representing SEs are included but are smaller than the markers (n = 3).

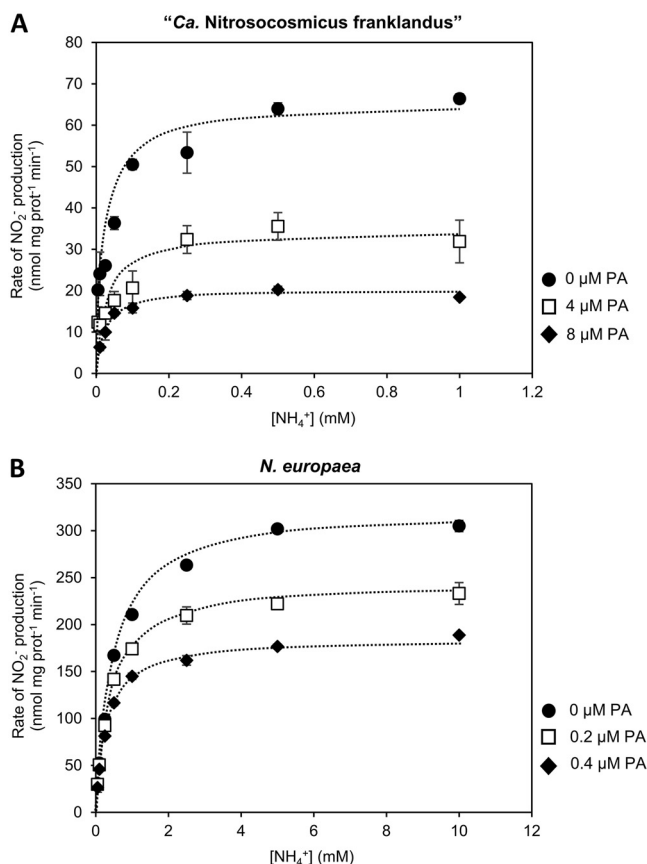


FIG 3 Michaelis-Menten hyperbolic plot showing the initial rate of NO_2^- production by *Ca. Nitrosocosmicus franklandus* (A) and *N. europaea* (B) to phenylacetylene (PA) dissolved in DMSO as a function of NH_4^+ concentration. The x axis is the substrate (NH_4^+) concentration and the y axis is the initial rate of NO_2^- production. Inhibition was not overcome by increasing concentration of NH_4^+ , indicating that phenylacetylene and NH_3 do not compete for the same binding site. Error bars represent SEs ($n = 3$).

NO_2^- production by *Ca. Nitrosocosmicus franklandus* was inhibited $55.4\% \pm 1.4\%$ in the presence of $5 \mu\text{M}$ phenylacetylene compared to that in the dimethyl sulfoxide (DMSO) control. Incubations in the presence of 10 and $20 \mu\text{M}$ phenylacetylene increased the inhibition to $74.7\% \pm 0.5\%$ and $86.0\% \pm 0.4\%$, respectively (Fig. 2A). NO_2^- production by *N. europaea* was inhibited $52.5\% \pm 1.7\%$ in the presence of $0.5 \mu\text{M}$ phenylacetylene, and unlike the results from Lontoh et al. (54), who showed full inhibition at $0.6 \mu\text{M}$, there was still partial NH_3 -oxidizing activity in the presence of $1 \mu\text{M}$ phenylacetylene ($75.1\% \pm 1.6\%$ inhibition on the rate of NO_2^- production) (Fig. 2B). Together, the results show that *Ca. Nitrosocosmicus franklandus* is approximately $10\times$ more resistant to phenylacetylene inhibition than *N. europaea*. Both *Ca. Nitrosocosmicus franklandus* and *N. europaea* cells incubated with 0.1% DMSO produced NO_2^- at a similar rate to that of untreated controls.

Kinetic analysis of phenylacetylene inhibition of NH_4^+ -dependent NO_2^- production by *Ca. Nitrosocosmicus franklandus* and *N. europaea*. To investigate the mode of inhibition of phenylacetylene on AMO, the initial reaction velocities of NO_2^- production by *Ca. Nitrosocosmicus franklandus* and *N. europaea* were determined over a range of substrate (total NH_4^+) concentrations. The concentrations of phenylacetylene used in the kinetic analysis were selected to achieve partial inhibition of NO_2^- production (Fig. 2). NH_3 -dependent kinetics of initial NO_2^- production followed Michaelis-Menten-type saturation kinetics for both *Ca. Nitrosocosmicus franklandus* and *N. europaea* (Fig. 3A and B), where the velocity (v) of the AMO-catalyzed reactions was hyperbolically related to the total NH_4^+ concentration ($[S]$):

TABLE 1 Kinetics of NH₃-dependent NO₂⁻ production by “*Ca. Nitrosocosmicus franklandus*” and *N. europaea* in the presence of phenylacetylene^a

Strain	Phenylacetylene (μM)	K _{m(app)} (μM)	V _{max(app)} (nmol mg protein ⁻¹ min ⁻¹)
“ <i>Ca. Nitrosocosmicus franklandus</i> ”	0	26.7 (4.7)	64.1 (2.6)
	4	30.3 (8.3)	33.8 (2.2)
	8	22.9 (3.2)	20.1 (0.5)
<i>N. europaea</i>	0	520.3 (19.6)	324.4 (3.7)
	0.2	375.3 (17.4)	240.7 (2.7)
	0.4	318.4 (13.8)	188.7 (2.0)

^aSEs of three replicates are in parentheses (*n* = 3).

$$v = \frac{V_{\max} \cdot [S]}{K_m + [S]}$$

Apparent half-saturation constants for total NH₄⁺ [K_{m(app)}] and maximum velocities [V_{max(app)}] in the presence/absence of phenylacetylene were calculated using hyperbolic regression analysis. The hyperbolic plots show that increasing the NH₄⁺ concentration did not alleviate the inhibitory effect of phenylacetylene on NO₂⁻ production in “*Ca. Nitrosocosmicus franklandus*” or *N. europaea* (Fig. 3A and B). This suggests that phenylacetylene is not a simple competitive inhibitor of either the archaeal or the bacterial AMO with respect to NH₃ oxidation. Interestingly, “*Ca. Nitrosocosmicus franklandus*” and *N. europaea* seem to have different mechanisms of inhibition by phenylacetylene. With “*Ca. Nitrosocosmicus franklandus*,” the presence of 4 and 8 μM phenylacetylene decreased the V_{max(app)} of NO₂⁻ production from 64.1 ± 2.6 nmol mg protein⁻¹ min⁻¹ to 33.8 ± 2.2 and 20.1 ± 0.5 nmol mg protein⁻¹ min⁻¹, respectively (Table 1). There was no significant change in the K_{m(app)} for cells inhibited by phenylacetylene compared to that for the control (*P* = 0.503 and *P* = 0.526 for 4 and 8 μM phenylacetylene, respectively), indicating that phenylacetylene and NH₃ do not compete for the same binding site. Inhibition of *N. europaea* by 0.2 and 0.4 μM phenylacetylene reduced both the K_{m(app)} and the V_{max(app)} by approximately 30% and 40%, respectively (Table 1). This is indicative of uncompetitive inhibition and suggests that phenylacetylene binds to AMO subsequent to NH₃ binding and at a different binding site.

Previously, acetylene was shown to be a competitive inhibitor of the archaeal AMO from *Nitrososphaera viennensis* (48). To examine if acetylene interacts competitively with “*Ca. Nitrosocosmicus franklandus*” AMO, the kinetic response of NH₃-dependent NO₂⁻ production by “*Ca. Nitrosocosmicus franklandus*” to 3 μM acetylene was tested using the same experimental design used to investigate phenylacetylene inhibition. In contrast to phenylacetylene, increasing the total NH₄⁺ availability reduced acetylene inhibition, demonstrating that acetylene and NH₃ compete for the same AMO binding site (see Fig. S2). Additionally, the K_{m(app)} increased dramatically from 18.5 ± 2.9 μM to 691.3 ± 158.1 μM NH₄⁺ in the presence of 3 μM acetylene, but there was no change in the V_{max(app)} (see Table S2), also demonstrating that acetylene interacts with the NH₃-binding site and decreases the affinity of AMO for NH₃.

Phenylacetylene was dissolved in 100% DMSO, and all cell suspensions used in both the phenylacetylene and acetylene experiments contained 0.1% (vol/vol) DMSO. Therefore, the effect of the addition of 0.1% (vol/vol) DMSO on NH₃ oxidation kinetics was tested separately. DMSO had no effect on kinetic parameters for NH₃ oxidation by “*Ca. Nitrosocosmicus franklandus*.” For *N. europaea*, the presence of 0.1% (vol/vol) DMSO reduced the K_{m(app)} and V_{max(app)} by approximately 10% (see Table S1).

Effect of phenylacetylene on hydroxylamine oxidation by “*Ca. Nitrosocosmicus franklandus*.” Hydroxylamine is the product of NH₃ oxidation by both the archaeal and bacterial AMOs and is subsequently oxidized to other intermediates in the NO₂⁻ production pathway (60, 61). To verify that the reduction in the rate of NO₂⁻ production by “*Ca. Nitrosocosmicus franklandus*” was due to inhibition of NH₃ oxidation rather

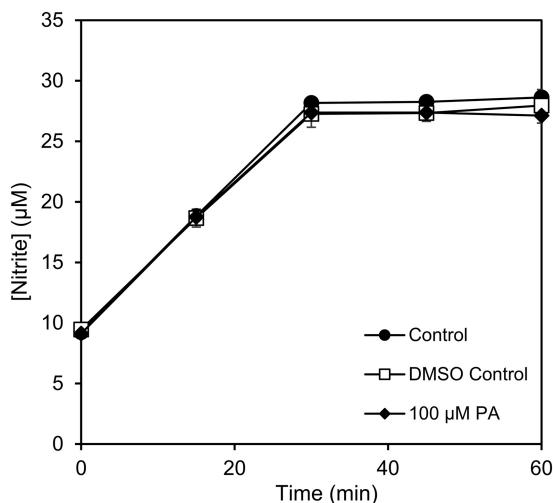


FIG 4 NO_2^- production from hydroxylamine oxidation by “*Ca. Nitrosocosmicus franklandus*” in the presence or absence of 100 μM phenylacetylene (PA) dissolved in DMSO. Error bars represent SEs ($n = 3$).

than the effects of downstream enzymatic reactions, we investigated hydroxylamine oxidation by “*Ca. Nitrosocosmicus franklandus*” in the presence of phenylacetylene. NO_2^- production by “*Ca. Nitrosocosmicus franklandus*” was unaffected by 100 μM phenylacetylene relative to the DMSO control treatment, demonstrating that phenylacetylene is likely a specific inhibitor of the AMO from “*Ca. Nitrosocosmicus franklandus*” (Fig. 4). Hydroxylamine-dependent NO_2^- production proceeded rapidly but ceased after 30 min when approximately 27 μM NO_2^- had accumulated. A similar response was previously observed for the marine AOA *Nitrosopumilus maritimus* SCM1 (60).

Recovery of AMO activity in “*Ca. Nitrosocosmicus franklandus*” following phenylacetylene inhibition. To establish whether phenylacetylene is a reversible or irreversible inhibitor of AMO from “*Ca. Nitrosocosmicus franklandus*,” the recovery of NH_3 -oxidizing activity after exposure to phenylacetylene was investigated. Previous work has shown that in order to restore AMO activity following inhibition by an irreversible inhibitor, for example, acetylene, cells need to synthesize new AMO enzyme, which results in a lag phase before activity resumes (42). “*Ca. Nitrosocosmicus franklandus*” cells were inhibited overnight by 100 μM phenylacetylene in the presence of 1 mM NH_4^+ . Since it was previously shown that inhibition by 1-octyne was reversible in the AOA *N. viennensis*, in contrast to the irreversible action of acetylene (48), treatments with both 1-octyne and acetylene were included as controls. To ensure that the inability of cells to respond to substrate addition (NH_4^+) was not due to the effects of starvation, controls incubated for a similar amount of time without either inhibitor or NH_4^+ were included (starved cells). After the removal of the inhibitors by washing, cells were resuspended in NH_4^+ -replete medium. NO_2^- production, the proxy for NH_3 oxidation, by “*Ca. Nitrosocosmicus franklandus*” recovered immediately following removal of 1-octyne. Cells inhibited by either acetylene or phenylacetylene had a 3- to 5-h lag time before NO_2^- production began, suggesting that cells required *de novo* synthesis of new AMO in order to oxidize NH_3 (Fig. 5). The starved cells recovered at the same rate as the controls (data not shown).

Cycloheximide is a potent inhibitor of protein synthesis in eukaryotes (62) and might be expected to have a similar effect in archaea. Previously, Vajjala et al. (63) demonstrated that it inhibited protein synthesis in the marine AOA, *N. maritimus* SCM1, preventing the recovery of NH_3 -oxidizing activity following inactivation of the AMO by acetylene. However, the same concentration range of cycloheximide did not prevent the recovery of NH_3 -oxidizing activity in *N. viennensis* following AMO inactivation with acetylene (48). Here, we observed that after complete inhibition by 20 μM acetylene, cycloheximide slowed, although it did not completely prevent, recovery of NH_3 -oxidizing activity by “*Ca. Nitrosocosmicus franklandus*” (see Fig. S3).

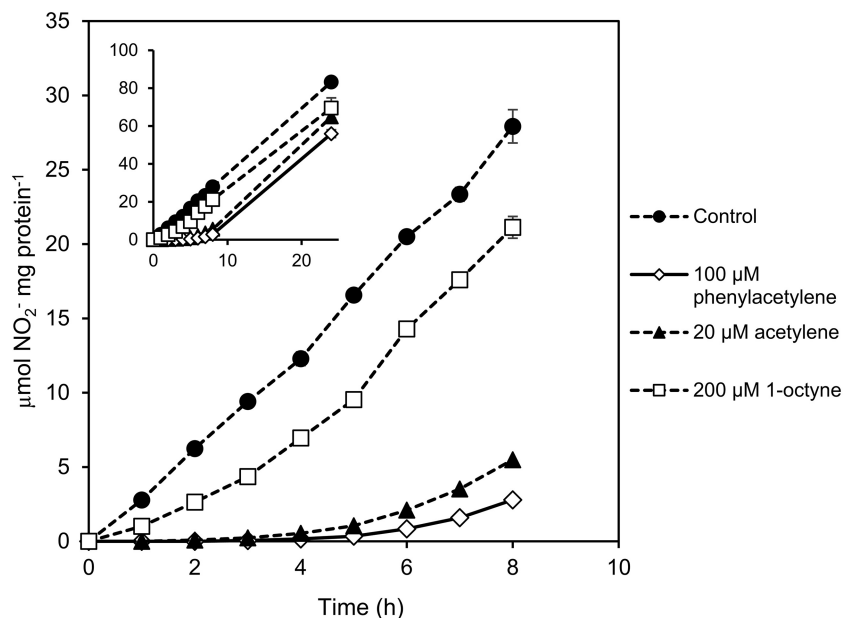


FIG 5 Time course of the recovery of NO_2^- production by *Ca. Nitrosocosmicus franklandus* following overnight inhibition of NH_3 oxidation by phenylacetylene (100 μM), acetylene (20 μM), and 1-octyne (200 μM). Error bars represent SEs ($n = 3$).

DISCUSSION

Inhibition of AMO and pMMO by linear alkynes. Linear terminal alkynes were previously shown to differentially inhibit archaeal and bacterial AMO activity (47, 48). In agreement with this, NH_3 -dependent NO_2^- production by the AOA strains *Ca. Nitrosocosmicus franklandus* and *Ca. Nitrosotalea sinensis* was considerably less sensitive to inhibition by longer-chain-length 1-alkynes ($\geq \text{C}_6$) compared to *N. europaea* (Fig. 1). The linear 1-alkyne inhibition profile appears to be conserved across AOA lineages, with the overall trend of increased sensitivity to short-chain alkynes and reduced sensitivity to longer-chain-length alkynes. This could indicate that, unlike the AMO from *N. europaea*, the binding cavity of the archaeal AMO cannot orientate and activate larger linear hydrocarbons such as 1-octyne, potentially due to steric hindrance caused by the bulkiness of these substrates or inhibitors. Interestingly, inhibition of the AMO from *Ca. Nitrosocosmicus franklandus* by 1-octyne, when used at 200 μM , was reversible, and recovery of NH_3 -oxidizing activity began immediately after removal of the inhibitor (Fig. 5). Similarly, Taylor et al. (48) showed the inhibition of AMO from *N. viennensis* by 1-octyne was also reversible.

In contrast with AOA, NH_3 oxidation by *N. europaea* was fully or partially inhibited by all C_2 to C_8 1-alkynes, with full inhibition occurring in the presence of longer-chain-length alkynes ($\geq \text{C}_6$). This is consistent with previous results published by Hyman et al. (21) and Taylor et al. (47) who found that long-chain-length 1-alkynes inhibited AMO of *N. europaea* more effectively than short-chain 1-alkynes. Additionally, it was observed by Hyman et al. (21) that the effectiveness of *n*-alkynes as inhibitors of AMO from *N. europaea* as the chain length increases. For example, 1-octyne inactivates *N. europaea* AMO more rapidly and effectively than shorter-chain-length 1-alkynes; however, the corresponding alkane, 1-octane, is oxidized more slowly and yields less product than short-chain alkanes (21).

The pMMO has a narrower hydrocarbon substrate range than the AMO of *N. europaea* but is capable of oxidizing short-chain *n*-alkanes ($\leq \text{C}_5$) and alkenes ($\leq \text{C}_3$) to their respective alcohols and epoxides (17). The specific site where hydrocarbon oxidation takes place within the pMMO is unclear. Intriguingly, a hydrophobic cavity identified in proximity to the predicted tricopper site in the PmoA from *M. capsulatus* (Bath) was shown to be of sufficient size to accommodate hydrocarbons of up to five

carbons in length (30, 64, 65). Correspondingly, here, we found that C₂ to C₅ alkynes inhibited the NH₃-oxidizing activity of pMMO from *M. capsulatus* (Bath) by more than 20%, reflecting the predicted size of this pMMO binding cavity (Fig. 1D). The inhibition of the pMMO by longer-chain alkynes (C₆ to C₈) was not previously tested, and we found that NH₃ oxidation by *M. capsulatus* (Bath) was marginally inhibited by C₆ and C₇ alkynes, indicating that the pMMO can interact with hydrocarbons with longer chain lengths than those already known to be substrates.

The effectiveness of C₂ to C₈ linear 1-alkynes as inhibitors of NH₃ oxidation by the AOA strains used in this study and in previous studies (47, 48) indicates that the archaeal AMO has a narrower hydrocarbon substrate range than the AMO of *N. europaea*. Furthermore, in terms of the 1-alkyne inhibition profile, the AMOs of "*Ca. Nitrosocosmicus franklandus*" and "*Ca. Nitrosotalea sinensis*" more closely resemble the pMMO from *M. capsulatus* (Bath) than the AMO of *N. europaea*. It could, therefore, be anticipated that the archaeal AMO oxidizes a similar range of linear *n*-alkanes and alkenes to that oxidized by the pMMO (Fig. 1).

Based on the diversity of archaeal AMO sequences (7), it is very likely that variation exists between the structure and stereoselectivity of the AMO active site from different AOA strains. Previously, Taylor et al. (47, 48) observed differences in the sensitivity of *N. maritimus*, *N. viennensis*, and "*Candidatus Nitrososphaera gargensis*" to inhibition by 1-hexyne (C₆) and 1-heptyne (C₇). In this study, we did not observe significant inhibition of archaeal AMO activity by 1-heptyne, although the AMO from "*Ca. Nitrosotalea sinensis*" was notably more sensitive to inhibition by C₂ to C₅ 1-alkynes than the AMO from "*Ca. Nitrosocosmicus franklandus*." Additionally, 1-hexyne had a significant inhibitory effect on NO₂⁻ production by "*Ca. Nitrosotalea sinensis*" but not by "*Ca. Nitrosocosmicus franklandus*" (Fig. 1A and B).

A considerable amount of research has focused on determining the environmental drivers influencing AOA and AOB ecology and their relative contribution to nitrification. Environmental factors, including substrate availability, pH, O₂ availability, and temperature, have been suggested to influence the ecological niche differentiation of ammonia oxidizers and to control ammonia oxidation rates in distinct ecosystems. The resistance of "*Ca. Nitrosocosmicus franklandus*" and "*Ca. Nitrosotalea sinensis*" to inhibition by 1-octyne (C₈) further justifies the use of 1-octyne to distinguish between AOA and AOB nitrifying activity in soils and to reveal the environmental factors influencing niche differentiation (49–51). Determining the patterns in the distributions of AOA and AOB in the environment could improve land and water management to mitigate negative impacts associated with nitrification.

Inhibition of AMO by phenylacetylene. Evidence from field studies indicated that phenylacetylene inhibited nitrification activity by AOA (53). Here, we examined phenylacetylene inhibition in pure culture with the terrestrial AOA strain "*Ca. Nitrosocosmicus franklandus*." Our data show that in "*Ca. Nitrosocosmicus franklandus*," phenylacetylene is a specific inhibitor of AMO, as it had no effect on hydroxylamine-dependent NO₂⁻ production (Fig. 4). Kinetic analysis suggested that phenylacetylene does not compete with NH₃ for the same AMO binding site, since increasing the substrate (NH₄⁺) concentration did not protect against inhibition (Fig. 3A). In contrast, higher concentrations of NH₄⁺ provided a protective effect when "*Ca. Nitrosocosmicus franklandus*" was incubated with acetylene, indicating acetylene and NH₃ compete for the same binding site (see Fig. S2 in the supplemental material). The recovery of AMO activity following complete inhibition by phenylacetylene incorporated a significant lag phase, similar to that observed for acetylene, suggesting that inhibition by these alkynes was irreversible and that cells required *de novo* protein synthesis of new AMO to reestablish NH₃-oxidizing activity (Fig. 5). Irreversible inhibition could indicate that the binding cavity of the AMO from "*Ca. Nitrosocosmicus franklandus*" is large enough to enable the orientation and subsequent activation of phenylacetylene and that phenylacetylene and acetylene essentially both act as suicide substrates. Curiously

though, our data suggest that phenylacetylene does not interact with the same binding site on AMO as NH_3 and acetylene.

Phenylacetylene is an irreversible inhibitor of AMO from *N. europaea* (41, 46). Here, we demonstrate that phenylacetylene does not compete with NH_3 for the same binding site (Fig. 3B). It has been proposed that the AMO from *N. europaea* may contain two distinct binding sites, one that specifically binds NH_3 and hydrocarbons $\leq \text{C}_3$ and a second that binds larger hydrocarbons, with oxidation occurring at either site (23, 45). Alternatively, different hydrocarbons might be able to access the active site of the AMO from two different directions (45). pMMO-expressing methanotrophs also exhibit complicated inhibition patterns when exposed to multiple hydrocarbon substrates. For example, dichloromethane acted as a competitive inhibitor of methane oxidation by *Methylosinus trichosporium* OB3b, but trichloromethane was best described as a non-competitive inhibitor, suggesting the existence of at least two substrate binding sites (20). Although the location and nuclearity of the active site for methane oxidation are still under debate, it is generally accepted that the pMMO contains multiple metal-binding sites, or potential active sites; therefore, it is possible that different hydrocarbons are oxidized at distinct sites on the pMMO. The noncompetitive nature of phenylacetylene inhibition, with respect to NH_3 , of the AMO from "*Ca. Nitrosocosmicus franklandus*" provides early indications either that distinct binding sites may be present on the archaeal AMO or that there are two separate routes by which substrates can access the archaeal AMO active site.

Kinetic analysis of phenylacetylene inhibition of AMO of "*Ca. Nitrosocosmicus franklandus*" and *N. europaea* revealed that phenylacetylene most likely interacts with the AMOs via distinct mechanisms. Specifically, phenylacetylene inhibition of AMO from *N. europaea* had characteristics of uncompetitive inhibition, where both the $K_{m(\text{app})}$ and $V_{\text{max}(\text{app})}$ decreased with increasing concentrations of phenylacetylene, indicating that the inhibitor only has affinity for the enzyme-substrate complex. Potentially, the binding of NH_3 induces a structural change in the AMO binding cavity, enabling phenylacetylene to bind at a putative secondary (non- NH_3) site. Phenylacetylene inhibition of the AMO from "*Ca. Nitrosocosmicus franklandus*" did not show the same characteristics as in *N. europaea* (Table 1), demonstrating that the interaction between phenylacetylene and the active site differed between the distinct AMO types.

Both AMO- and pMMO-expressing microorganisms have gained interest for their potential use in bioremediation due to their capability to cooxidize persistent organic pollutants such as halogenated alkanes and alkenes and chlorinated hydrocarbons (66, 67). Unlike the bacterial AMO, the oxidation of aromatic compounds has not been observed by the pMMO (17, 21, 45, 56). Lontoh et al. (54) showed that pMMOs from *M. capsulatus* (Bath) and several other strains of methanotrophs were relatively resistant to phenylacetylene inhibition, with whole-cell pMMO activity still present at 1 mM phenylacetylene. It is possible that aromatic compounds are simply too bulky to gain access to or be orientated at the pMMO active site (64). Although *N. europaea* appears to lack the ability to completely mineralize aromatic pollutants, it may initiate the degradation of aromatic compounds and provide oxidation products that can be transformed by other microorganisms (24). There is evidence that the archaeal AMO, unlike the pMMO, is capable of transforming aromatic compounds. Recently, Men et al. (68) demonstrated that the AOA strain "*Ca. Nitrososphaera gargensis*" was capable of cometabolizing two tertiary amines, mianserin and ranitidine, with the initial oxidative reaction most likely carried out by the AMO. Given that AOA have a significantly higher substrate affinity than AOB (69), AOA might be more effective in the biotransformation of some organic pollutants.

This research offers new insights into the structures and substrate ranges of AMOs from archaea using alkyne inhibitors in comparison with that of other members of the CuMMO family. Future studies should investigate the inhibitory effect and subsequent cooxidation of potential archaeal AMO substrates. Examining alternative substrate reactions and products could provide information about archaeal AMO stereoselectiv-

ity, advance our understanding of the enzyme structure, and improve predicted structural models for archaeal AMO.

MATERIALS AND METHODS

Materials. Phenylacetylene (98%) and propyne, 1-pentyne, 1-hexyne, 1-heptyne, and 1-octyne (C_3 , C_5 , C_6 , C_7 , and C_8 linear 1-alkynes, respectively, $\geq 97\%$) were obtained from Sigma-Aldrich. 1-Butyne was supplied by Apollo Gases Ltd. Acetylene was obtained from BOC, a member of the Linde Group. Protein concentrations were determined using a Pierce bicinchoninic acid (BCA) protein assay kit (Thermo Scientific) as described by the manufacturer.

Growth of cultures. “*Candidatus Nitrosotalea sinensis*” Nd2 and “*Candidatus Nitrosocosmicus franklandus*” C13 (70, 71) were grown as follows. “*Ca. Nitrosocosmicus franklandus*” was cultivated in freshwater medium (FWM) buffered with 10 mM HEPES (pH 7.5) and supplemented with 4 mM NH_4Cl as previously described (71). The acidophilic AOA “*Ca. Nitrosotalea sinensis*” was cultivated in FWM buffered with 2.5 mM morpholineethanesulfonic acid (MES; pH 5.3) and supplemented with 400 μM NH_4Cl as previously described (70). Both “*Ca. Nitrosocosmicus franklandus*” and “*Ca. Nitrosotalea sinensis*” were grown in 800-ml volumes in 1-liter Duran bottles incubated statically in the dark at 37°C. *Nitrosomonas europaea* ATCC 19718 was obtained from the University of Aberdeen culture collection and cultivated in 200-ml volumes, in 500-ml conical flasks, shaking (160 rpm) at 30°C in modified Skinner and Walker (72) medium (pH ~ 7.5) containing 0.235 g liter $^{-1}$ $(NH_4)_2SO_4$, 0.2 g liter $^{-1}$ KH_2PO_4 , 0.04 g liter $^{-1}$ $CaCl_2 \cdot 2H_2O$, 0.04 g liter $^{-1}$ $MgSO_4 \cdot 7H_2O$, and 0.3 mg liter $^{-1}$ FeNa-EDTA, buffered with 10 mM HEPES (pH 7.5), and 5% (wt/vol) Na_2CO_3 . *Methylococcus capsulatus* (Bath) was grown in 50-ml volumes in 250-ml Quickfit conical flasks, shaking (180 rpm) at 37°C in nitrate mineral salts (NMS) supplemented with 20 μM copper to promote pMMO expression under a CH_4 atmosphere of 40%. To confirm that *M. capsulatus* cells were only expressing pMMO and not soluble MMO (sMMO), the naphthalene assay, which is specific for sMMO activity, was used (73) with sMMO-expressing *Methylocella silvestris* cells as positive controls. The AOA strains “*Ca. Nitrosocosmicus franklandus*” and “*Ca. Nitrosotalea sinensis*” are available upon request.

Nitrite assay. NO_2^- concentrations were determined colorimetrically in a 96-well format using Griess reagent as previously described (70). Absorbance measurements were performed at a 540-nm wavelength using a VersaMax microplate reader (Molecular Devices).

Inhibition of whole cells by alkynes. “*Ca. Nitrosocosmicus franklandus*” and “*Ca. Nitrosotalea sinensis*” were cultivated to mid-exponential phase (~ 600 to 700 μM and ~ 80 to 90 μM NO_2^- accumulated, respectively), and 1,600 ml was harvested by filtration onto nucleopore 0.2- μm membrane filters (PALL). “*Ca. Nitrosocosmicus franklandus*” cells were washed and resuspended in 200 ml 10 mM HEPES (pH 7)-buffered FWM salts to $\sim 2 \times 10^7$ cells/ml. “*Ca. Nitrosotalea sinensis*” cells were washed and resuspended in 100 ml 2.5 mM MES (pH 5.3)-buffered FWM salts to $\sim 3 \times 10^7$ cells/ml. *N. europaea* was grown to mid-exponential phase, and a 400-ml culture was harvested by filtration, washed, and resuspended to $\sim 3 \times 10^7$ cells/ml in 200 ml 50 mM sodium phosphate buffer (pH 7.7) containing 2 mM $MgCl_2$ (12). *M. capsulatus* cells were grown to an optical density at 540 nm (OD_{540}) of 0.8, and 100 ml was harvested by centrifugation (14,000 $\times g$, 10 min). Cells were washed and resuspended in 50 ml 10 mM piperazine-*N,N'*-bis(2-ethanesulfonic acid) (PIPES) buffer (pH 7) to $\sim 2 \times 10^8$ cells/ml. Cells were rested for 1 h at their respective growth temperatures to achieve a baseline for enzyme activity assays. Aliquots of 5 ml “*Ca. Nitrosocosmicus franklandus*,” *N. europaea*, and *M. capsulatus* and 4 ml “*Ca. Nitrosotalea sinensis*” cell suspension were added to acid-washed 23-ml glass vials, which were then sealed with gray butyl rubber stoppers which had been autoclaved two times to remove contaminating substances. C_2 to C_8 linear 1-alkynes were added to the headspace as vapor to achieve a 10 μM aqueous concentration (C_{aq}), calculated using the Henry’s law coefficients obtained from Sander (74). Phenylacetylene was dissolved in 100% dimethyl sulfoxide (DMSO) to achieve various stock solutions. A final volume of 5 μl stock solution was added to cell suspensions, resulting in 0.1% (vol/vol) DMSO plus the desired concentration of phenylacetylene. Preliminary experiments determined that the addition of 0.1% (vol/vol) DMSO did not affect NH_4^+ -oxidizing activity (data not shown), and control treatments containing 0.1% (vol/vol) DMSO without phenylacetylene or acetylene were included. Cells were preincubated with inhibitors for 30 min to allow for the gas-liquid phase partitioning of the alkynes, at 37°C for “*Ca. Nitrosocosmicus franklandus*,” “*Ca. Nitrosotalea sinensis*,” and *M. capsulatus* and at 30°C for *N. europaea*. Total inorganic ammonium (NH_3 plus NH_4^+), referred to as NH_4^+ , was then added as NH_4Cl or $(NH_4)_2SO_4$ (reflecting the growth medium) to initiate NH_3 -oxidizing activity, and vials were incubated at the respective growth temperatures of the microorganisms. *M. capsulatus* was incubated with shaking (150 rpm). AMO and pMMO activity was determined by assaying NO_2^- production from NH_3 oxidation. NO_2^- production was measured and quantified as described above by withdrawing a sample of culture through the septum every 15 min for 2 h unless otherwise stated. All treatments were carried out in triplicates, and experiments were performed at least three times with similar results.

Sensitivity of isolates to C_2 to C_8 1-alkynes. C_2 to C_8 linear 1-alkynes were added to vials using a gas tight syringe. To initiate NH_3 oxidation by “*Ca. Nitrosocosmicus franklandus*,” *N. europaea*, and “*Ca. Nitrosotalea sinensis*,” NH_4^+ was added to a concentration of 1 mM by injection through the septum. For *M. capsulatus* (Bath), sodium formate was added first, as a source of reductant, immediately followed by NH_4^+ , both at a final concentration of 20 mM.

Sensitivity of “*Ca. Nitrosocosmicus franklandus*” and *N. europaea* to phenylacetylene. Phenylacetylene was added to achieve concentrations ranging from 2.5 to 20 μM for “*Ca. Nitrosocosmicus franklandus*” and 0.5 to 10 μM for *N. europaea*. To initiate ammonia oxidation, NH_4^+ was added to final concentrations of 0.5 mM and 5 mM to “*Ca. Nitrosocosmicus franklandus*” and *N. europaea*, respectively. NO_2^- production was measured for 60 min.

Relationship between NH_4^+ oxidation and phenylacetylene inhibition kinetics of “*Ca. Nitrosocosmicus franklandus*” and *N. europaea*. To determine NH_3 oxidation kinetics in the presence of phenylacetylene, “*Ca. Nitrosocosmicus franklandus*” and *N. europaea* cells were harvested and resuspended as described above, but to final concentrations of 1×10^7 and 8×10^6 cells/ml, respectively. “*Ca. Nitrosocosmicus franklandus*” cell suspensions were preincubated with phenylacetylene (0, 4, or 8 μM) or acetylene (0 or 3 μM) for 30 min before the addition of various concentrations of NH_4^+ (0.005 to 1 mM). *N. europaea* cell suspensions were preincubated with phenylacetylene (0, 0.2, or 0.4 μM) before the addition of 0.05 to 10 mM NH_4^+ . Additional experiments were carried out to test the effect of 0.1% (vol/vol) DMSO on NH_3 oxidation kinetics by “*Ca. Nitrosocosmicus franklandus*” and *N. europaea* (see Table S1 in the supplemental material).

Phenylacetylene inhibition of hydroxylamine oxidation by “*Ca. Nitrosocosmicus franklandus*.” “*Ca. Nitrosocosmicus franklandus*” cell suspensions were incubated with 0 or 100 μM phenylacetylene. Hydroxylamine was added at a concentration of 200 μM , and hydroxylamine-dependent NO_2^- production was measured over 60 min as described above.

Recovery of AMO activity from “*Ca. Nitrosocosmicus franklandus*” following phenylacetylene inhibition. “*Ca. Nitrosocosmicus franklandus*” cells were grown to mid-exponential phase, and 3,200 ml was harvested by filtration as described above and concentrated into 70 ml FWM containing 10 mM HEPES (pH 7.5). Aliquots of 5 ml cell suspension were added to glass vials and sealed with butyl rubber seals. Phenylacetylene (100 μM) and 1-octyne (200 μM) were added from DMSO stock solutions (as described above), and acetylene (20 μM) was added from a 1% (vol/vol in air) gaseous stock. Both control and acetylene treatments also contained 0.1% (vol/vol) DMSO. The addition of NH_4^+ (1 mM) initiated NH_3 -oxidizing activity and vials were incubated at 37°C overnight (16 h). NO_2^- production was monitored for 1 h to assess baseline activity. To remove inhibitors and test AMO recovery, samples were pooled into 50-ml Falcon tubes, and the cells were washed three times in FWM containing 10 mM HEPES (pH 7.5) by centrifugation ($12,000 \times g$ for 10 min at 5°C). The pellet was resuspended in 700 μl FWM containing 10 mM HEPES (pH 7.5). Aliquots (200 μl) of cell suspension were added to 4.8 ml FWM containing 10 mM HEPES (pH 7.5) plus 1 mM NH_4^+ , resulting in a final cell concentration of $\sim 1.3 \times 10^7$ cells/ml. Vials were incubated in a water bath (37°C), and NO_2^- production was monitored over 24 h.

Statistics. Linear 1-alkyne data were plotted as average activity as a fraction of the control treatments (no inhibitor). To analyze phenylacetylene inhibition kinetics, the initial rates of NO_2^- production were plotted against NH_4^+ concentration. A nonlinear regression was used to estimate the $K_{m(\text{app})}$ and $V_{\text{max}(\text{app})}$ for NH_4^+ using the Hyper32 kinetics package. Significant differences between treatments were identified by one-way analysis of variance (ANOVA) with Dunnett’s (2-sided) *post hoc* test (IBM SPSS version 25).

SUPPLEMENTAL MATERIAL

Supplemental material is available online only.

SUPPLEMENTAL FILE 1, PDF file, 0.5 MB.

ACKNOWLEDGMENTS

L.E.L.-M. is funded by a Royal Society Dorothy Hodgkin Research Fellowship (DH150187) and by a European Research Council (ERC) Starting Grant (UNITY 852993). C.L.W. is funded by a University of East Anglia-funded PhD studentship. A.S. is funded by a Royal Society Dorothy Hodgkin Fellowship Enhancement Award (RGF\EA\180300). A.T.C. is funded by a Leverhulme Trust Early Career Fellowship (ECF-2016-626).

We thank Tom Clarke for valuable discussion on the analysis of the kinetics data.

REFERENCES

- Daims H, Lebedeva EV, Pjevac P, Han P, Herbold C, Albertsen M, Jehmlich N, Palatinszky M, Vierheilig J, Bulaev A, Kirkegaard RH, von Bergen M, Rattei T, Bendinger B, Nielsen PH, Wagner M. 2015. Complete nitrification by *Nitrospira* bacteria. *Nature* 528:504–509. <https://doi.org/10.1038/nature16461>.
- Van Kessel MA, Speth DR, Albertsen M, Nielsen PH, den Camp HJO, Kartal B, Jetten MS, Lückner S. 2015. Complete nitrification by a single microorganism. *Nature* 528:555–559. <https://doi.org/10.1038/nature16459>.
- Lehtovirta-Morley LE. 2018. Ammonia oxidation: ecology, physiology, biochemistry and why they must all come together. *FEMS Microbiol Lett* 365:fny058. <https://doi.org/10.1093/femsle/fny058>.
- Leininger S, Urlich T, Schlöter M, Schwark L, Qi J, Nicol GW, Prosser JI, Schuster SC, Schleper C. 2006. Archaea predominate among ammonia-oxidizing prokaryotes in soils. *Nature* 442:806–809. <https://doi.org/10.1038/nature04983>.
- Wuchter C, Abbas B, Coolen MJ, Herfort L, van Bleijswijk J, Timmers P, Strous M, Teira E, Herndl GJ, Middelburg JJ, Schouten S, Sinninghe Damsté JS. 2006. Archaeal nitrification in the ocean. *Proc Natl Acad Sci U S A* 103:12317–12322. <https://doi.org/10.1073/pnas.0600756103>.
- Francis CA, Beman JM, Kuypers MM. 2007. New processes and players in the nitrogen cycle: the microbial ecology of anaerobic and archaeal ammonia oxidation. *ISME J* 1:19–27. <https://doi.org/10.1038/ismej.2007.8>.
- Alves RJE, Minh BQ, Urlich T, von Haeseler A, Schleper C. 2018. Unifying the global phylogeny and environmental distribution of ammonia-oxidising archaea based on *amoA* genes. *Nat Commun* 9:1517. <https://doi.org/10.1038/s41467-018-03861-1>.
- Lawton TJ, Ham J, Sun T, Rosenzweig AC. 2014. Structural conservation of the B subunit in the ammonia monooxygenase/particulate methane monooxygenase superfamily. *Proteins* 82:2263–2267. <https://doi.org/10.1002/prot.24535>.
- Lancaster KM, Caranto JD, Majer SH, Smith MA. 2018. Alternative bioenergy: updates to and challenges in nitrification metalloenzymology. *Joule* 2:421–441. <https://doi.org/10.1016/j.joule.2018.01.018>.
- Holmes AJ, Costello A, Lidstrom ME, Murrell JC. 1995. Evidence that participate methane monooxygenase and ammonia monooxygenase may be evolutionarily related. *FEMS Microbiol Lett* 132:203–208. [https://doi.org/10.1016/0378-1097\(95\)00311-r](https://doi.org/10.1016/0378-1097(95)00311-r).

11. Pester V, Schleper C, Wagner M. 2011. The Thaumarchaeota: an emerging view of their phylogeny and ecophysiology. *Curr Opin Microbiol* 14:300–306. <https://doi.org/10.1016/j.mib.2011.04.007>.
12. Hyman MR, Wood PM. 1983. Methane oxidation by *Nitrosomonas europaea*. *Biochem J* 212:31–37. <https://doi.org/10.1042/bj2120031>.
13. Ward BB. 1987. Kinetic studies on ammonia and methane oxidation by *Nitrosococcus oceanus*. *Arch Microbiol* 147:126–133. <https://doi.org/10.1007/BF00415273>.
14. Dalton H. 1977. Ammonia oxidation by the methane oxidising bacterium *Methylococcus capsulatus* strain Bath. *Arch Microbiol* 114:273–279. <https://doi.org/10.1007/BF00446873>.
15. O'Neill JG, Wilkinson JF. 1977. Oxidation of ammonia by methane-oxidizing bacteria and the effects of ammonia on methane oxidation. *J Gen Microbiol* 100:407–412. <https://doi.org/10.1099/00221287-100-2-407>.
16. Nyerges G, Stein LY. 2009. Ammonia cometabolism and product inhibition vary considerably among species of methanotrophic bacteria. *FEMS Microbiol Lett* 297:131–136. <https://doi.org/10.1111/j.1574-6968.2009.01674.x>.
17. Burrows KJ, Cornish A, Scott D, Higgins IJ. 1984. Substrate specificities of the soluble and particulate methane mono-oxygenases of *Methylosinus trichosporium* OB3b. *J Gen Microbiol* 130:3327–3333. <https://doi.org/10.1099/00221287-130-12-3327>.
18. Bédard C, Knowles R. 1989. Physiology, biochemistry, and specific inhibitors of CH₄, NH₄⁺, and CO oxidation by methanotrophs and nitrifiers. *Microbiol Mol Biol Rev* 53:68–84. <https://doi.org/10.1128/MMBR.53.1.68-84.1989>.
19. Miyaji A, Miyoshi T, Motokura K, Baba T. 2011. The substrate binding cavity of particulate methane monooxygenase from *Methylosinus trichosporium* OB3b expresses high enantioselectivity for *n*-butane and *n*-pentane oxidation to 2-alcohol. *Biotechnol Lett* 33:2241–2246. <https://doi.org/10.1007/s10529-011-0688-3>.
20. Lontoh S, DiSpirito AA, Semrau JD. 1999. Dichloromethane and trichloroethylene inhibition of methane oxidation by the membrane-associated methane monooxygenase of *Methylosinus trichosporium* OB3b. *Arch Microbiol* 171:301–308. <https://doi.org/10.1007/s002030050714>.
21. Hyman MR, Murton IB, Arp DJ. 1988. Interaction of ammonia monooxygenase from *Nitrosomonas europaea* with alkanes, alkenes, and alkynes. *Appl Environ Microbiol* 54:3187–3190. <https://doi.org/10.1128/AEM.54.12.3187-3190.1988>.
22. Rasche ME, Hyman MR, Arp DJ. 1991. Factors limiting aliphatic chloro-carbon degradation by *Nitrosomonas europaea*: cometabolic inactivation of ammonia monooxygenase and substrate specificity. *Appl Environ Microbiol* 57:2986–2994. <https://doi.org/10.1128/AEM.57.10.2986-2994.1991>.
23. Keener WK, Arp DJ. 1993. Kinetic studies of ammonia monooxygenase inhibition in *Nitrosomonas europaea* by hydrocarbons and halogenated hydrocarbons in an optimized whole-cell assay. *Appl Environ Microbiol* 59:2501–2510. <https://doi.org/10.1128/AEM.59.8.2501-2510.1993>.
24. Keener WK, Arp DJ. 1994. Transformations of aromatic compounds by *Nitrosomonas europaea*. *Appl Environ Microbiol* 60:1914–1920. <https://doi.org/10.1128/AEM.60.6.1914-1920.1994>.
25. Hyman MR, Kim CY, Arp DJ. 1990. Inhibition of ammonia monooxygenase in *Nitrosomonas europaea* by carbon disulfide. *J Bacteriol* 172:4775–4782. <https://doi.org/10.1128/jb.172.9.4775-4782.1990>.
26. Juliette LY, Hyman MR, Arp DJ. 1993. Inhibition of ammonia oxidation in *Nitrosomonas europaea* by sulfur compounds: thioethers are oxidized to sulfoxides by ammonia monooxygenase. *Appl Environ Microbiol* 59:3718–3727. <https://doi.org/10.1128/AEM.59.11.3718-3727.1993>.
27. Lieberman RL, Rosenzweig AC. 2005. Crystal structure of a membrane-bound metalloenzyme that catalyses the biological oxidation of methane. *Nature* 434:177–182. <https://doi.org/10.1038/nature03311>.
28. Walker CB, De La Torre JR, Klotz MG, Urakawa H, Pinel N, Arp DJ, Brochier-Armanet C, Chain PSG, Chan PP, Gollabgir A, Hemp J, Hügl M, Karr EA, Könneke M, Shin M, Lawton TJ, Lowe T, Martens-Habbena W, Sayavedra-Soto LA, Lang D, Sievert SM, Rosenzweig AC, Manning G, Stahl DA. 2010. *Nitrosopumilus maritimus* genome reveals unique mechanisms for nitrification and autotrophy in globally distributed marine crenarchaea. *Proc Natl Acad Sci U S A* 107:8818–8823. <https://doi.org/10.1073/pnas.0913533107>.
29. Martinho M, Choi DW, DiSpirito AA, Antholine WE, Semrau JD, Münck E. 2007. Mössbauer studies of the membrane-associated methane monooxygenase from *Methylococcus capsulatus* Bath: evidence for a diiron center. *J Am Chem Soc* 129:15783–15785. <https://doi.org/10.1021/ja077682b>.
30. Chan SI, Yu S. 2008. Controlled oxidation of hydrocarbons by the membrane-bound methane monooxygenase: the case for a tricopper cluster. *Acc Chem Res* 41:969–979. <https://doi.org/10.1021/ar700277n>.
31. Cao L, Calderaru O, Rosenzweig AC, Ryde U. 2018. Quantum refinement does not support dinuclear copper sites in crystal structures of particulate methane monooxygenase. *Angew Chem Int Ed Engl* 57:162–166. <https://doi.org/10.1002/anie.201708977>.
32. Lu Y-J, Hung M-C, Chang BT-A, Lee T-L, Lin Z-H, Tsai I-K, Chen Y-S, Chang C-S, Tsai Y-F, Chen KH-C, Chan SI, Yu SS-F. 2019. The PmoB subunit of particulate methane monooxygenase (pMMO) in *Methylococcus capsulatus* (Bath): the CuI sponge and its function. *J Inorg Biochem* 196:110691. <https://doi.org/10.1016/j.jinorgbio.2019.04.005>.
33. Ross MO, MacMillan F, Wang J, Nisthal A, Lawton TJ, Olafson BD, Mayo SL, Rosenzweig AC, Hoffman BM. 2019. Particulate methane monooxygenase contains only mononuclear copper center centers. *Science* 364:566–570. <https://doi.org/10.1126/science.aav2572>.
34. Ro SY, Schachner LF, Koo CW, Purohit R, Remis JP, Kenney GE, Liauw BW, Thomas PM, Patrie SM, Kelleher NL, Rosenzweig AC. 2019. Native top-down mass spectrometry provides insights into the copper centers of membrane-bound methane monooxygenase. *Nature Commun* 10:2675. <https://doi.org/10.1038/s41467-019-10590-6>.
35. Hooper AB, Terry KR. 1973. Specific inhibitors of ammonia oxidation in *Nitrosomonas*. *J Bacteriol* 115:480–485. <https://doi.org/10.1128/JB.115.2.480-485.1973>.
36. Taylor AE, Zeglin LH, Dooley S, Myrold DD, Bottomley PJ. 2010. Evidence for different contributions of archaea and bacteria to the ammonia-oxidizing potential of diverse Oregon soils. *Appl Environ Microbiol* 76:7691–7698. <https://doi.org/10.1128/AEM.01324-10>.
37. Lehtovirta-Morley LE, Verhamme DT, Nicol GW, Prosser JI. 2013. Effect of nitrification inhibitors on the growth and activity of *Nitrosotalea devanatterra* in culture and soil. *Soil Biol Biochem* 62:129–133. <https://doi.org/10.1016/j.soilbio.2013.01.020>.
38. Shen T, Stieglmeier M, Dai J, Ulrich T, Schleper C. 2013. Responses of the terrestrial ammonia-oxidizing archaea *Ca. Nitrososphaera viennensis* and the ammonia-oxidizing bacterium *Nitrosospira multiformis* to nitrification inhibitors. *FEMS Microbiol Lett* 344:121–129. <https://doi.org/10.1111/1574-6968.12164>.
39. Hynes RK, Knowles R. 1982. Effect of acetylene on autotrophic and heterotrophic nitrification. *Can J Microbiol* 28:334–340. <https://doi.org/10.1139/m82-049>.
40. Prior SD, Dalton H. 1985. Acetylene as a suicide substrate and active site probe for methane monooxygenase from *Methylococcus capsulatus* (Bath). *FEMS Microbiol Lett* 29:105–109. <https://doi.org/10.1111/j.1574-6968.1985.tb00843.x>.
41. Hyman MR, Wood PM. 1985. Suicidal inactivation and labelling of ammonia mono-oxygenase by acetylene. *Biochem J* 227:719–725. <https://doi.org/10.1042/bj2270719>.
42. Hyman MR, Arp DJ. 1992. ¹⁴C₂H₂- and ¹⁴CO₂-labeling studies of the *de novo* synthesis of polypeptides by *Nitrosomonas europaea* during recovery from acetylene and light inactivation of ammonia monooxygenase. *J Biol Chem* 267:1534–1545.
43. McTavish HJ, Fuchs JA, Hooper AB. 1993. Sequence of the gene coding for ammonia monooxygenase in *Nitrosomonas europaea*. *J Bacteriol* 175:2436–2444. <https://doi.org/10.1128/jb.175.8.2436-2444.1993>.
44. Gilch S, Vogel M, Lorenz MW, Meyer O, Schmidt I. 2009. Interaction of the mechanism-based inactivator acetylene with ammonia monooxygenase of *Nitrosomonas europaea*. *Microbiology* 155:279–284. <https://doi.org/10.1099/mic.0.023721-0>.
45. Keener WK, Russell SA, Arp DJ. 1998. Kinetic characterization of the inactivation of ammonia monooxygenase in *Nitrosomonas europaea* by alkyne, aniline and cyclopropane derivatives. *Biochim Biophys Acta* 1388:373–385. [https://doi.org/10.1016/s0167-4838\(98\)00188-5](https://doi.org/10.1016/s0167-4838(98)00188-5).
46. Bennett K, Sadler NC, Wright AT, Yeager C, Hyman MR. 2016. Activity-based protein profiling of ammonia monooxygenase in *Nitrosomonas europaea*. *Appl Environ Microbiol* 82:2270–2279. <https://doi.org/10.1128/AEM.03556-15>.
47. Taylor AE, Vajrala N, Giguere AT, Gitelman AI, Arp DJ, Myrold DD, Sayavedra-Soto L, Bottomley PJ. 2013. Use of aliphatic *n*-alkynes to discriminate soil nitrification activities of ammonia-oxidizing thaumarchaea and bacteria. *Appl Environ Microbiol* 79:6544–6551. <https://doi.org/10.1128/AEM.01928-13>.
48. Taylor AE, Taylor K, Tennigkeit B, Palatinszky M, Stieglmeier M, Myrold DD, Schleper C, Wagner M, Bottomley PJ. 2015. Inhibitory effects of C₂ to

- C₁₀ 1-alkynes on ammonia oxidation in two *Nitrososphaera* species. *Appl Environ Microbiol* 81:1942–1948. <https://doi.org/10.1128/AEM.03688-14>.
49. Lu X, Bottomley PJ, Myrold DD. 2015. Contributions of ammonia-oxidizing archaea and bacteria to nitrification in Oregon forest soils. *Soil Biol Biochem* 85:54–62. <https://doi.org/10.1016/j.soilbio.2015.02.034>.
 50. Taylor AE, Giguere AT, Zobebelein CM, Myrold DD, Bottomley PJ. 2017. Modeling of soil nitrification responses to temperature reveals thermodynamic differences between ammonia-oxidizing activity of archaea and bacteria. *ISME J* 11:896–908. <https://doi.org/10.1038/ismej.2016.179>.
 51. Giguere AT, Taylor AE, Suwa Y, Myrold DD, Bottomley PJ. 2017. Uncoupling of ammonia oxidation from nitrite oxidation: impact upon nitrous oxide production in non-cropped Oregon soils. *Soil Biol Biochem* 104:30–38. <https://doi.org/10.1016/j.soilbio.2016.10.011>.
 52. Hink L, Nicol GW, Prosser JI. 2017. Archaea produce lower yields of N₂O than bacteria during aerobic ammonia oxidation in soil. *Environ Microbiol* 19:4829–4837. <https://doi.org/10.1111/1462-2920.13282>.
 53. Im J, Lee SW, Bodrossy L, Barcelona MJ, Semrau JD. 2011. Field application of nitrogen and phenylacetylene to mitigate greenhouse gas emissions from landfill cover soils: effects on microbial community structure. *Appl Microbiol Biotechnol* 89:189–200. <https://doi.org/10.1007/s00253-010-2811-0>.
 54. Lontoh S, DiSpirito AA, Krema CL, Whittaker MR, Hooper AB, Semrau JD. 2000. Differential inhibition *in vivo* of ammonia monooxygenase, soluble methane monooxygenase and membrane-associated methane monooxygenase by phenylacetylene. *Environ Microbiol* 2:485–494. <https://doi.org/10.1046/j.1462-2920.2000.00130.x>.
 55. Vannelli T, Hooper AB. 1995. NIH shift in the hydroxylation of aromatic compounds by the ammonia-oxidizing bacterium *Nitrosomonas europaea*. Evidence against an arene oxide intermediate. *Biochem* 34:11743–11749. <https://doi.org/10.1021/bi00037a011>.
 56. Colby J, Stirling DI, Dalton H. 1977. The soluble methane monooxygenase of *Methylococcus capsulatus* (Bath). Its ability to oxygenate *n*-alkanes, *n*-alkenes, ethers, and alicyclic, aromatic and heterocyclic compounds. *Biochem J* 165:395–402. <https://doi.org/10.1042/bj1650395>.
 57. Campbell MA, Nyerges G, Kozlowski JA, Poret-Peterson AT, Stein LY, Klotz MG. 2011. Model of the molecular basis for hydroxylamine oxidation and nitrous oxide production in methanotrophic bacteria. *FEMS Microbiol Lett* 322:82–89. <https://doi.org/10.1111/j.1574-6968.2011.02340.x>.
 58. Suzuki I, Dular U, Kwok SC. 1974. Ammonia or ammonium ion as substrate for oxidation by *Nitrosomonas europaea* cells and extracts. *J Bacteriol* 120:556–558. <https://doi.org/10.1128/JB.120.1.556-558.1974>.
 59. Lehtovirta-Morley LE, Sayavedra-Soto LA, Gallois N, Schouten S, Stein LY, Prosser JI, Nicol GW. 2016. Identifying potential mechanisms enabling acidophily in the ammonia-oxidizing archaeon *Candidatus Nitrosotalea devanaterrea*. *Appl Environ Microbiol* 82:2608–2619. <https://doi.org/10.1128/AEM.04031-15>.
 60. Vajrala N, Martens-Habbena W, Sayavedra-Soto LA, Schauer A, Bottomley PJ, Stahl DA, Arp DJ. 2013. Hydroxylamine as an intermediate in ammonia oxidation by globally abundant marine archaea. *Proc Natl Acad Sci U S A* 110:1006–1011. <https://doi.org/10.1073/pnas.1214272110>.
 61. Caranto JD, Lancaster KM. 2017. Nitric oxide is an obligate bacterial nitrification intermediate produced by hydroxylamine oxidoreductase. *Proc Natl Acad Sci U S A* 114:8217–8222. <https://doi.org/10.1073/pnas.1704504114>.
 62. Siegel MR, Sisler HD. 1963. Inhibition of protein synthesis *in vitro* by cycloheximide. *Nature* 200:675–676. <https://doi.org/10.1038/200675a0>.
 63. Vajrala N, Bottomley PJ, Stahl DA, Arp DJ, Sayavedra-Soto LA. 2014. Cycloheximide prevents the *de novo* polypeptide synthesis required to recover from acetylene inhibition in *Nitrosopumilus maritimus*. *FEMS Microbiol Ecol* 88:495–502. <https://doi.org/10.1111/1574-6941.12316>.
 64. Ng KY, Tu LC, Wang YS, Chan SI, Yu S. 2008. Probing the hydrophobic pocket of the active site in the particulate methane monooxygenase (pMMO) from *Methylococcus capsulatus* (Bath) by variable stereoselective alkane hydroxylation and olefin epoxidation. *Chembiochem* 9:1116–1123. <https://doi.org/10.1002/cbic.200700628>.
 65. Culpepper MA, Rosenzweig AC. 2012. Architecture and active site of particulate methane monooxygenase. *Crit Rev Biochem Mol Biol* 47:483–492. <https://doi.org/10.3109/10409238.2012.697865>.
 66. Sayavedra-Soto LA, Gvakharia B, Bottomley PJ, Arp DJ, Dolan ME. 2010. Nitrification and degradation of halogenated hydrocarbons—a tenuous balance for ammonia-oxidizing bacteria. *Appl Microbiol Biotechnol* 86:435–444. <https://doi.org/10.1007/s00253-010-2454-1>.
 67. Semrau J. 2011. Bioremediation via methanotrophy: overview of recent findings and suggestions for future research. *Front Microbiol* 2:209. <https://doi.org/10.3389/fmicb.2011.00209>.
 68. Men Y, Han P, Helbling DE, Jehmlich N, Herbold C, Gulde R, Onnis-Hayden A, Gu AZ, Johnson DR, Wagner M, Fenner K. 2016. Biotransformation of two pharmaceuticals by the ammonia-oxidizing archaeon *Nitrososphaera gargensis*. *Environ Sci Technol* 50:4682–4692. <https://doi.org/10.1021/acs.est.5b06016>.
 69. Martens-Habbena W, Berube PM, Urakawa H, de la Torre JR, Stahl DA. 2009. Ammonia oxidation kinetics determine niche separation of nitrifying *Archaea* and *Bacteria*. *Nature* 461:976–979. <https://doi.org/10.1038/nature08465>.
 70. Lehtovirta-Morley LE, Ge C, Ross J, Yao H, Nicol GW, Prosser JI. 2014. Characterisation of terrestrial acidophilic archaeal ammonia oxidisers and their inhibition and stimulation by organic compounds. *FEMS Microbiol Ecol* 89:542–552. <https://doi.org/10.1111/1574-6941.12353>.
 71. Lehtovirta-Morley LE, Ross J, Hink L, Weber EB, Gubry-Rangin C, Thion C, Prosser JI, Nicol GW. 2016. Isolation of '*Candidatus Nitrosocosmicus franklandus*', a novel ureolytic soil archaeal ammonia oxidiser with tolerance to high ammonia concentration. *FEMS Microbiol Ecol* 92:fiw057. <https://doi.org/10.1093/femsec/fiw057>.
 72. Skinner FA, Walker N. 1961. Growth of *Nitrosomonas europaea* in batch and continuous culture. *Arch Mikrobiol* 38:339–349. <https://doi.org/10.1007/BF00408008>.
 73. Brusseau GA, Tsien HC, Hanson RS, Wackett LP. 1990. Optimization of trichloroethylene oxidation by methanotrophs and the use of a colorimetric assay to detect soluble methane monooxygenase activity. *Bio-degradation* 1:19–29. <https://doi.org/10.1007/bf00117048>.
 74. Sander R. 2015. Compilation of Henry's law constants (version 4.0) for water as solvent. *Atmos Chem Phys* 15:4399–4981. <https://doi.org/10.5194/acp-15-4399-2015>.